104 (2025) 105059

Contents lists available at ScienceDirect

Poultry Science

journal homepage: www.elsevier.com/locate/psj

Full-Length Article

Cadmium disrupted homeostasis of proximal renal tubular cells via targeting ATF4-CHOP complex into the nucleus

Muhammad Asmat Ullah Saleem [a,1], Ying-Xin Zhao [a,1], Farhat Bano [a,1], Yi-Xi Tang [a], Mu-Zi Li [a], Kanwar Kumar Malhi [a], Xiao-Wei Li [a], Xue-Nan Li [a,b,c], Yi Zhao [a,b,c], Jin-Long Li [a,b,c,*]

[a] College of Veterinary Medicine, Northeast Agricultural University, Harbin, 150030, PR China
[b] Key Laboratory of the Provincial Education Department of Heilongjiang for Common Animal Disease Prevention and Treatment, Northeast Agricultural University, Harbin, 150030, PR China
[c] Heilongjiang Key Laboratory for Laboratory Animals and Comparative Medicine, Northeast Agricultural University, Harbin, 150030, PR China

ARTICLE INFO

Keywords:
Cadmium
Kidney
Homeostasis
Nephrotoxicity
ATF4-CHOP axis

ABSTRACT

Cadmium, a ubiquitous toxic metal and environmental pollutant, is associated with several renal metabolic disorders and disrupts the homeostasis of kidneys in humans and animals. However, the precise molecular mechanism remains poorly elucidated. The present study investigated the role of the ATF4-CHOP nuclear transcriptional axis and its interactions with cellular pathways in cadmium-induced nephrotoxicity. We acquired 120 one-day-old chickens, randomly divided them into four groups (Con, Cd35, Cd70, Cd140), and were treated with graded cadmium doses for 90 days. The kidney tissues were collected for comprehensive histopathological, biochemical, and molecular analyses using western blotting, qRT-PCR, immunofluorescence, and tunel assay. Subsequently, we revealed that cadmium exposure induced ER stress, significantly upregulated CHOP expression, and activated pro-apoptotic ATF4-CHOP axis. Our findings revealed a complex interplay, where ER stress activated inflammation. Concurrently, mitochondrial disruption elevated ROS production and oxidative stress, which impaired renal homeostasis. Moreover, inhibition of autophagy and mitophagy led to the accumulation of damaged cell organelles, further exacerbating apoptotic signaling. Our results elucidate that an integrated network of cellular stress pathways mediates cadmium-induced renal toxicity, with the ATF4-CHOP axis acting as a crucial pro-apoptotic pathway. This study provides critical insights into the mechanisms of cadmium-induced nephrotoxicity and potential therapeutic interventions to mitigate heavy metal-induced renal homeostasis disruption and renal damage.

Interoduction

Cadmium (**Cd**) is a non-essential toxic heavy metal and environmental pollutant that poses significant global hazards to human and animal health (Bautista et al., 2024; Wróblewski et al., 2024). Cd is widely used in industries such as pesticides, plastics, pigments, electroplating, and nickel cadmium-batteries production and causes pollution in natural environments such as soil, surface water and food (Doccioli et al., 2024; Kaya and Yalçın, 2024; Zhang et al., 2023). The European Commission has stipulated a maximum permissible Cd concentration in poultry kidneys of 1.0 mg/kg (No, 2021). Cd is highly toxic owing to its non-biodegradable nature and half-life of 10-30 years (Guo et al., 2024; Rahman et al., 2023). Cd can enter the body through food chain, accumulate in the body through systematic circulation, and ultimately damage to several organs and tissues, including the kidneys, testicles, liver, lungs, and bones. However, kidney is the primary target organ of Cd-exposure (Bronner et al., 2015; Ding et al., 2024; Kaya and Yalçın, 2024). Several studies have demonstrated that Cd exposure has been associated with various health issues, including kidney disease, atherosclerosis, osteoporosis, neurodegenerative disorders, cardiovascular and pulmonary diseases (Ma et al., 2022; Zhao et al., 2024). Previous studies reported that Cd disrupts endoplasmic reticulum (**ER**) homeostasis and triggers the accumulation of misfolded proteins (Kaya and Yalçın, 2024; Wu et al., 2023; Zhang et al., 2024b). Furthermore,

* Corresponding author at: College of Veterinary Medicine, Northeast Agricultural University, Harbin, 150030, PR China.
E-mail address: Jinlongli@neau.edu.cn (J.-L. Li).
[1] These authors contributed equally to this study.

https://doi.org/10.1016/j.psj.2025.105059
Received 16 February 2025; Accepted 17 March 2025
Available online 18 March 2025

Cd-induced mitochondrial dysfunction disrupts mitochondrial dynamics, impairs energy production, and promotes apoptosis through cytochrome c release and caspase-3 activation (Ansari et al., 2017; Cui et al., 2023; Dong et al., 2024; Huang et al., 2022; Zhang et al., 2024a). Approximately 50 % of Cd deposition occurs in proximal convoluted tubules, triggering renal dysfunction and chronic kidney disorder (Fujiki et al., 2024; Ijaz et al., 2023; Jung and Oh, 2022; Li et al., 2024).

Despite the significant impact of Cd exposure, lack of comprehensive knowledge concerning its nephrotoxic effects in chicken kidneys remains limited. Proximal renal tubular cells are located in the renal cortical region and are the key sites of Cd accumulation and subsequent renal toxicity (Gu et al., 2018). These specialized epithelial cells, which line the proximal convoluted tubules of the nephron, are highly susceptible to Cd-induced damage and dysfunction owing to their direct exposure to Cd-containing glomerular filtration. These cells' strategic location and functional significance within the nephron critical targets for investigating the mechanisms of Cd-induced renal damage (Vesey, 2010) Recent data indicate that transcriptional regulation mediated by activating transcription factor 4 (**ATF4**) and C/EBP homologous protein (**CHOP**) axis plays a critical role in Cd-induced apoptosis of proximal renal tubular cells (Mori et al., 2022). Furthermore, Cd-induced ER stress response has been shown to activate ATF4-CHOP axis, which plays a crucial role in the ER stress-mediated apoptosis in proximal renal tubular cells (Zou et al., 2024). However, the specific molecular mechanisms by which Cd influences this transcriptional ATF4-CHOP axis and its targets require further research to fully explain the pathogenesis of Cd-induced renal damage.

This study aimed to explain existing research gaps by focusing on Cd-induced damage to proximal renal tubular cells in chickens. Although previous investigations provided a broader perspective on Cd toxicity, our research explores the precise cellular mechanisms of renal homeostasis disruption. Chickens serve as excellent experimental models for studying Cd-induced nephrotoxicity owing to their heightened sensitivity to Cd, especially in renal tissues. Chickens are widely used in toxicology research due to their availability, ease of handling, and ability to maintain controlled environmental and dietary conditions during the experimental period. Therefore, chickens were chosen as experimental animals for this experiment. We identified that Cd exposure disrupted ER homeostasis and induced mitochondrial dysfunction in proximal renal tubular cells, triggering a cascade of pathological changes. TEM analysis revealed autophagosome formation, highlighting impaired autophagy as a critical factor contributing to cellular stress and apoptosis. Additionally, mechanistic studies have shown that ATF4-CHOP axis plays a key role in this process. ATF4-CHOP forms a complex in the nucleus that interferes with transcriptional processes, ultimately activating cellular apoptosis. The molecular docking analysis demonstrated that Cd promotes the formation of complex with a binding energy of - 2.8 kJ/mol. This study will provide an inclusive understanding of the molecular mechanism of Cd nephrotoxicity in the avian model and identify potential future interventions to mitigate renal damage.

Materials and methods

Ethical approval and experimental design

The study's experimental procedures and animal care were performed according to the Guidelines for Care and Use of Laboratory Animals of Northeast Agricultural University (**NEAU**), Harbin, P.R. China. Furthermore, all animal experiments comply with the institutional animal care and use committee (**IACUC**) and Northeast Agricultural University Care and Ethics Committee (NEAUEC20200346) guidelines. A total of 120 male Hylin-White chickens (1-day-old) were acquired from Xian Feng Chick Farm (Harbin, China), and randomly allocated into four groups: Control (**Con**) and Cd (Cd35mg/kg, Cd70mg/kg, Cd140mg/kg) exposure groups. This experiment involved 30 chickens in each group. We adapt group-housed method. The experimental design and feeding plan are summarized in Fig. S1. We used chicken feed No. 511, which was purchased from Zhengda Company, China. The specific ingredients were corn 55.3 %, soybean meal 38 %, dicalcium phosphate 1.4 %, stone powder 1 %, salt 0.3 %, oil 3 %, and additive 1 %. After 90 days, chickens were kept under fasting for 12 h and then euthanized. The kidney tissues were carefully removed and stored at -80 °C for further analysis.

Chemical reagents and dose selection

Cadmium chloride (**$CdCl_2$**, CAS: 10108-64-2, >99.0 %) was supplied by Tianjin Zhi-yuan Chemical Reagent Company, Tianjin, China. Cd exposure induces ER stress, mitochondrial dysfunction, autophagy/mitophagy dysregulation, inflammation, and apoptosis in kidney cells. The obtained median lethal dose (**LD**) of Cd (LD50) was 218.55 mg/kg BW/day. Sub-chronic daily Cd doses were set at 35 mg/kg feed (3/20 LD50), 70 mg/kg (3/10 LD50), and 140 mg/kg (3/5 LD50) for 90 days to investigate dose-dependent effects on kidney function. This study observed that highest adverse effects were after exposure to 140 mg/kg (Li et al., 2023; Sun et al., 2022; Talukder et al., 2021)

Determination of kidney functions

Cd exposure affects kidney functions. Renal biochemical markers were assess from serum isolated from whole blood to quantify blood urea nitrogen (**BUN**), creatinine (**CREA**), and Uric Acid (**UA**) levels by using commercial kits according to manufacturer guidelines (SINOWA, P.R. China). Data were analyzed using a biochemical auto-analyzer (Shenzhen, P.R. China).

Histopathological analysis

Histopathological analysis was performed according to the previous method for microstructure assessment (Li et al., 2024). After 90 days, kidney tissues were collected and immediately fixed in 10 % neutral-buffer formalin. Briefly, following the standard hematoxylin-eosin (**H&E**) staining protocol, tissues were dehydrated with a gradient series of an alcohol, embedded in paraffin wax, 5 μm tissue sections were trimmed, stained with H&E staining and covered with glass slips. The images were acquired, and visualized the renal histological structures under a light microscope.

Ultrastructural analysis via transmission electron microscopy

Kidney tissues for ultrastructure analysis were prepared. Briefly, renal tissues ($1 \times 1 \times 1$;$n = 5$/group) were quickly fixed in 2.5 % glutaraldehyde at 4°C overnight, washed with PBS buffer solution, post-fixed in osmium tetroxide, and embedded in ethoxy resin. After dehydration and waxing, thin sections were trimmed. The sections were visualized under a transmission electron microscope (Hitachi H-7650 TEM Tokyo, Japan). The mitochondrial score and ER stress were calculated. ER-mitochondrial volume densities were determined and nuclear scoring was conducted through semi-quantitative analysis, employing methods outlined in earlier research (Jiang et al., 2024).

Immunofluorescence staining of ATF4 and CHOP

Immunofluorescence (**IF**) staining was used to analyze ATF4 and CHOP co-localization in kidney tissue. Briefly, we followed the standard protocol of IF double-labeled staining. The ATF4 (CAT#GB111137 Servicebio) and CHOP (CAT #GB115691, Servicebio) antibodies were purchased from Servicebio (Wuhan-Hubei, China). Images were acquired using a Leica-DMi8 microscope. Representative IF staining images of ATF4 (Red) and CHOP (green) with DAPI (blue) nuclear counterstain staining as a negative control. Quantification analysis of

the IF-positive index (intensity) was performed using Image J software. Details of the procedure in **Supplementary 1.1.**

TUNEL assay

To investigate apoptosis, terminal deoxynucleotidyl transferase dUTP nick end labeling (**TUNEL**) assay was performed. Kidney samples were de-paraffinized using xylene, rehydrated through a graded alcohol series, and washed with distilled water. After 15-minute digestion with 20 μg/mL proteinase K, the sections were rinsed twice with phosphate-buffered saline (PBS). Next, samples were incubated in an equilibration buffer for 10 s before adding dUTP digoxigenin and concentrated TdT from the TUNEL assay kit. This mixture was incubated for 1 h at 37 °C in a humidified chamber for dUTP digoxigenin incorporation. After the reaction, the sections were incubated in the dark for 30 min with an anti-digoxigenin antibody. Finally, the tissue sections were mounted under coverslips and visualized using a confocal laser scanning microscope (Talukder et al., 2021; Zhao et al., 2021, 2023)

Protein extraction and western blotting

Total proteins were extracted from kidney tissues (0.1g) for western blot analysis by homogenization of 250 μL mixture that contained protease inhibitor cocktail (MedChem, Express, USA) and RIPA lysis buffer (Beyotime, Shanghai, China) at a ratio of 1:100. The homogenate mixture was centrifuged at 12000 g (4 °C) for 15 min. The supernatant was collected to prepare a final concentration of 5 μg/μL of total protein by adding 1 × PBS and 5 × sample loading buffer. The mixture was boiled at 98 °C for 10 min in a water-bath and cooled at room temperature to obtain total-proteins. The nuclear proteins were extracted using a commercial kit (Jiancheng-Bio, Jiangsu P.R China) protocol explained in our previous studies (Chen et al., 2023) . Proteins were separated by SDS-PAGE (12 - 15 % separated gels) and then transferred to nitrocellulose (**NC**) membranes (Biosharp, PR., China). NC- membranes were blocked for 1 h with 5 % PBS free-fat milk solution at 37°C for 75 min, incubated with diluted primary antibody overnight at 4°C, and then incubated with secondary antibody for 1 h at 37 °C (HRP-labeled, Goat Anti-Rabbit IgG, 1:3000, Santa, Cruz, USA). Lamin-β and β-actin antibodies were used as controls for normalization. The protein band intensities were evaluated using the Amersham-600 imager. Finally, Image J software was used to quantify protein densities. Details of antibodies used in this study is given Table 1.

Table 1
Details of antibodies used in this study.

Name of the antibody	Name of the company	Dilution
β-actin	Beijing Biosynthesis Biotechnology Co. Ltd, Beijing, China	1:800
Lamin B	Beijing Biosynthesis Biotechnology Co. Ltd, Beijing, China	1:600
GRP78	ABclonal Technology, Wuhan, China	1:800
PERK	ABclonal Technology, Wuhan, China	1:800
eIF-2α	ABclonal Technology, Wuhan, China	1:600
ATF4	Affinity Biosciences, Jiangsu, China	1.500
CHOP	ABclonal Technology, Wuhan, China	1:800
XBP1	ABclonal Technology, Wuhan, China	1.800
ATF6	Affinity Biosciences, Jiangsu, China	1.600
Beclin1	ABclonal Technology, Wuhan, China	1.800
LC3B	ABclonal Technology, Wuhan, China	1.1000
p62	ABclonal Technology, Wuhan, China	1.1000
Mfn1	ABclonal Technology, Wuhan, China	1.800
Mfn2	ABclonal Technology, Wuhan, China	1.800
OPA1	Bioss, Beijing Boaosen, Biotechnology, Co. Ltd, Beijing, China	1.500
Drp1	ABclonal Technology, Wuhan, China	1.800
PINK1	ABclonal Technology, Wuhan, China	1.800
TNF-α	ABclonal Technology, Wuhan, China	1:800
IL-10	Affinity Biosciences, Jiangsu, China	1:600
Bcl2	Wanleibio, China	1:800
Bax	Wanleibio, China	1:800
Bak	Wanleibio, China	1:600
Casp-3	Bioss, Beijing Boaosen, Biotechnology, Co. Ltd, Beijing, China	1.500
Casp-8	ABclonal Technology, Wuhan, China	1:800
Casp-9	ABclonal Technology, Wuhan, China	1.800
(HRP)-conjugated goat anti-rabbit(IgG) secondary antibody	Santa Cruz, CA, USA	1:3000

Total RNA extraction and RT-qPCR analysis

Total RNA was extracted from kidney tissue using the RNAout commercial kit (Tiandz, Inc., Beijing, China), following the manufacturers protocol. RNA concentration was determined using a UV spectrophotometer (GE, USA) by measuring the optical density at 260/280 nm. Samples with absorbance values between 1.8 and 2.1 were selected for RT-qPCR analysis. cDNA synthesis was performed using TranScript reverse transcriptase (TransGen, Biotech Co., Beijing, China) and a commercial kit containing Go-Taq® master mix (Promega, USA). Real-time PCR reactions were conducted using QuanStudio-5 Real-Time PCR (Thermo-Fisher Sci, USA). Specific primers were designed using Oligo 7.22 software (Molecular Biology Insights, USA), and their sequences are provided in Table S4. Primer specificity was confirmed by evaluating dissociation curves, which exhibited single peaks. The relative expression of mRNA was calculated using the $2^{-\triangle\triangle CT}$ method, with β-actin 1 and 2 used for normalization of cDNA. Details of primers sequence of qRT-PCR is provided in *Supplementary 1.2*.

Molecular docking

The protein structures of ATF4, CHOP, and the chemical structure of $CdCl_2$, were downloaded from the RCSB PDB database (https://www.rcsb.org) and the PubChem database (http://pubchem.ncbi.nlm.nih.gov/), respectively. Based on these compound structures, the protein-ligand docking was performed between ATF4, CHOP, and $CdCl_2$, using AutoDock 4.2. Moreover, the molecular docking results were further demonstrated by using the PyMol molecular visualizer software. Binding free energy was calculated to evaluate the interactions between the proteins and the ligand.

*Protein –Protein interactions (**PPI**) network and sequence analysis*

The target genes were analyzed using String Database (https://string-db-or/) website to identify the differentially expressed genes (**GEGs**) to PPI, which can predict functional protein interactions for differentially expressed proteins (DEPs).

PCA and correlation analysis

PCA and Correlation analysis plots were created using Origin Pro 2024.

Statistical analysis

All data analyses were executed using GraphPad Prism 8.0. The one-way analysis of variance (**ANOVA**) was carried out using the Graphpad Prism 8.0 software (GraphPad Software, America). Data were expressed as Heat maps, and Principal Component Analysis (**PCA**) plots were designed using OriginPro2024. Graphical Abstract was designed using www.biorender.com. PPI for protein networks using the String Database (https://sring-db-or/) to GEGs for predicting PPI.

Results

Cd-induced proximal renal tubular cell damage

This study demonstrated that Cd exposure induced proximal renal tubular cell damage. The experimental design, diet plan from day 0 to 90, and the groups were shown in Fig. S1. Histopathological analysis exhibited significant structural changes in kidney tissue, such as tubular dilations and glomerular damage, in Cd-induced groups as compared to the Con group (Fig. 1A). We measured glomerulus damages score, which exhibited higher damages scores in the Cd70, Cd140 groups (Fig. 1B, $P < 0.001$), and the tubular width measurements showed an obvious change in Cd70 group and a highly significant increase in the Cd 140 group (Fig. S1, $P < 0.001$), indicating progressive structural damage with higher Cd doses. The serum biomarkers, BUN, CREA, and UA were evaluated for renal function. Notably, BUN, CREA, and UA levels were significantly elevated in Cd140 group (Fig. 1C–E, $P < 0.001$) compared to Con group. The heatmap demonstrated that all indicators were significantly elevated in the Cd140 group (Fig. 1F). The illustration represented the anatomy of the proximal convoluted tubular cells of the kidney (Fig. 1G).

Cd-induced ER stress in proximal renal tubular cells

Numerous previous studies have demonstrated that ER plays a critical role in various cellular processes, therefore, we investigated ER stress activation in the kidney in response to Cd toxicity. Western blotting revealed a significant increase in UPR-related proteins (Fig. 2A). Notably, GRP78 protein levels were higher in the Cd70 ($P < 0.01$) and Cd140 groups (Fig. 2B, $P < 0.001$) as compared to Con group. Correspondingly, PERK activation was pronounced in Cd140 group (Fig. 2C, $P < 0.001$), which was correlated with increased expression of the downstream target protein elF-2α in all Cd groups (Fig. 2E, $P < 0.001$). The pro-apoptotic transcription factor CHOP was also significantly upregulated (Fig. 2D, $P < 0.001$) in Cd70 and Cd140 groups. Similarly, in comparison with Con group, ATF4 and ATF6 levels were significantly increased in Cd140 group (Fig. 2F, $P < 0.001$) and (Fig. 2G, $P < 0.001$) respectively. Further, XBP-1 protein expression was increased significantly in Cd140 group (Fig. 2H, $P < 0.001$). Furthermore, heatmap analysis of mRNA levels for key UPR-related genes (*Bip/GRP78, PERK, elF2α, CHOP, IRE1α, ATF4, ATF6, XBP1*) confirmed these findings that mRNA expression results were consistent with protein levels (Fig. 2I, S2). The parametric analysis of UPR-related proteins was performed using PCA, which further confirmed that Cd triggered ER stress and activated UPR (Fig. 2J). Schematic illustration demonstrated that Cd caused ER stress and activates URP in chicken kidneys (Fig. 2K). These findings indicated that Cd exposure induced ER-stress and activated the UPR in proximal renal tubular cells, with CHOP-ATF4 playing a crucial role in this entire process.

Cd-induced mitochondrial dynamics and autophagy

ER stress can cause protein misfolding and excessive accumulation of misfolded proteins leading to autophagy. Autophagosome formation

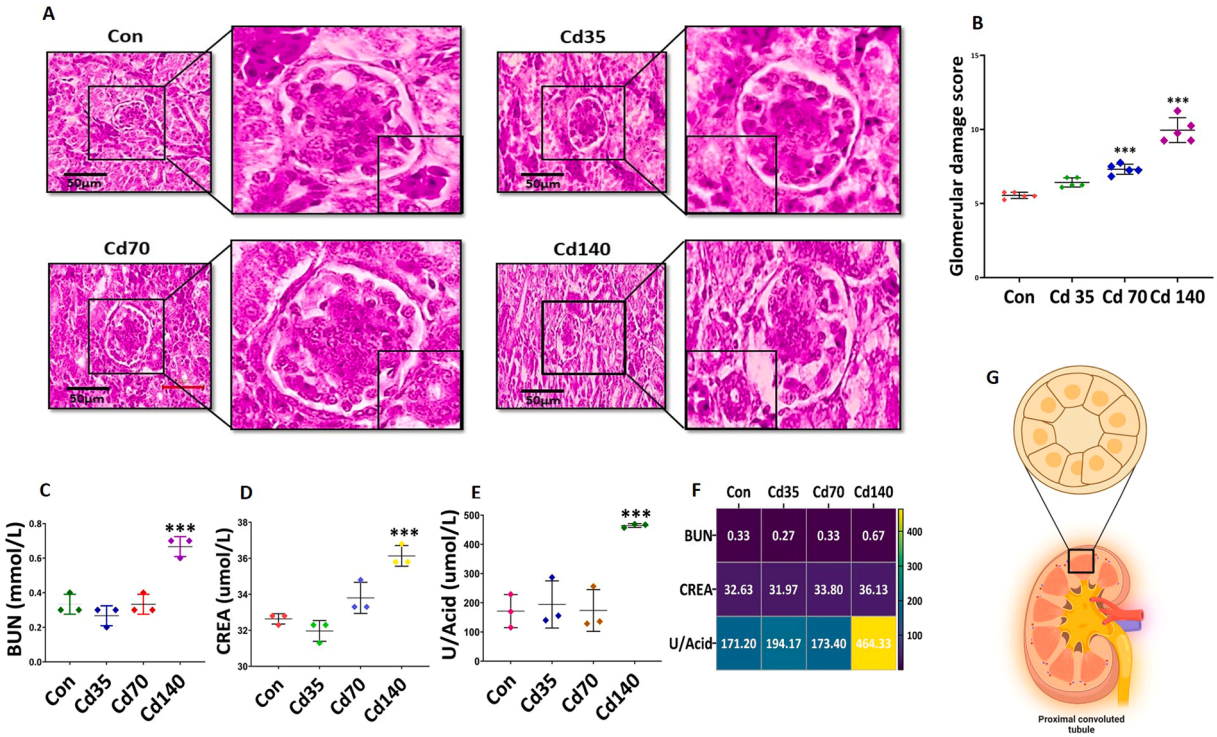

Fig. 1. Cd-induced proximal renal tubular cell damage. (A) Histopathological demonstration of proximal renal tubular cell under Cd exposure. (B) Quantification of glomerular damage score. (C) Blood Urea Nitrogen (BUN) levels. (D) Creatinine (CREA) levels. (E) Uric Acid levels. (F) Heatmap summary of kidney function markers. (G) The illustration represented the anatomy of the proximal convoluted tubular cells of the kidney. Histopathological demonstration of hematoxylin and eosin staining (200x and 400 x) of kidney section in different groups (Con, Cd35, Cd70, and Cd140) scale bar: 50 μm. Statistical data are presented as mean ± SD, ($n = 6$) symbol for the significance of difference between Con and other Cd exposed groups $^{*}P < 0.05$, $^{**}P < 0.01$, $^{***}P < 0.001$.

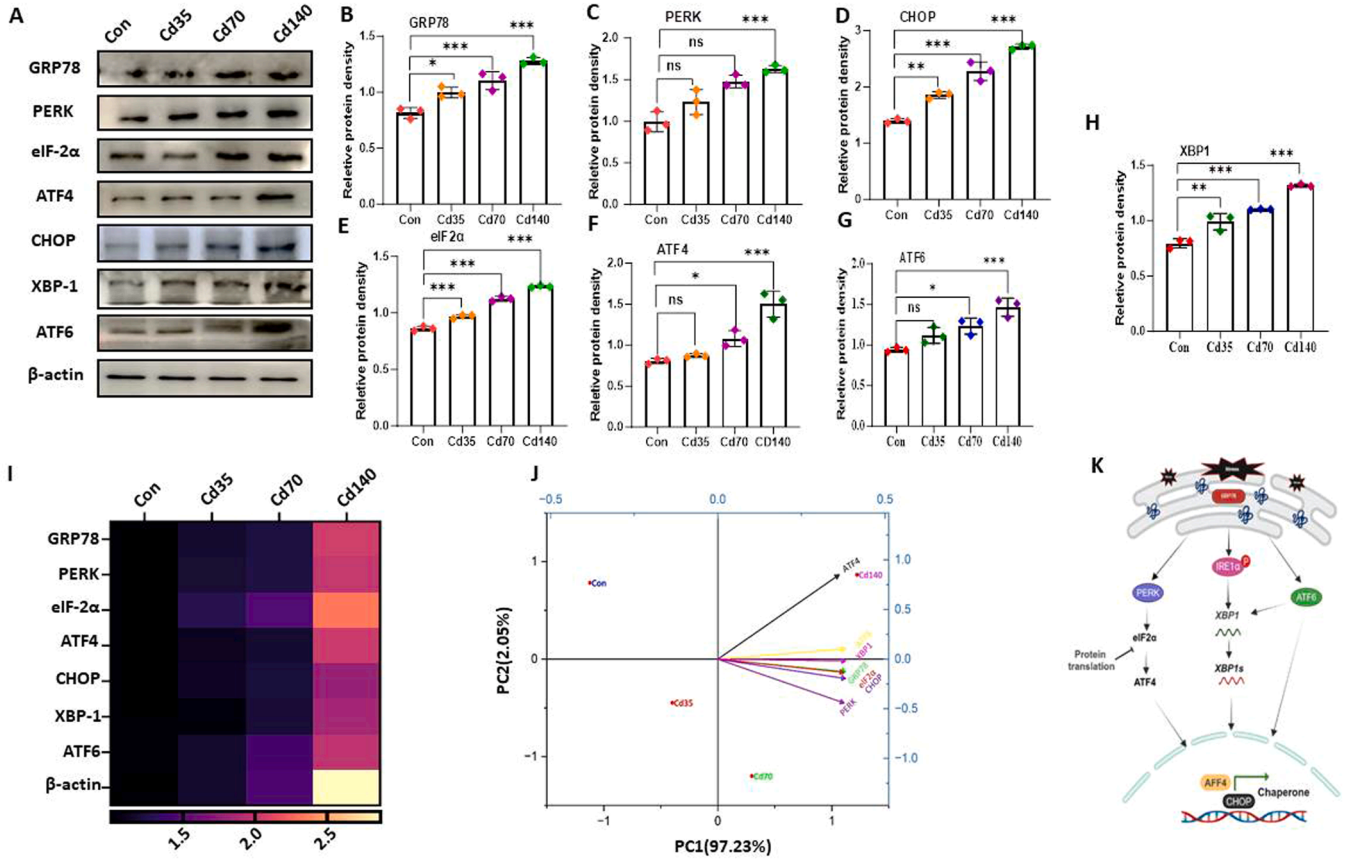

Fig. 2. Cd induced ER stress and activated URP. (A-H) Western blotting protein levels and quantification of relative protein densities of ER stress markers GRP78, PERK1, eIF2α, ATF4, CHOP, ATF6, and XBP-1. (I) Heatmap representation of relative mRNA expressions of UPR-related proteins. (J) Principal Component Analysis (PCA). (K) URP pathway image. Statistical data are presented as mean ± SD. Symbols for the significance of difference between Con and other Cd exposed groups: $^{*}P < 0.05$, $^{**}P < 0.01$, $^{***}P < 0.001$.

was observed in ultrastructural analysis, which indicated the activation of autophagic processes in Cd-treated kidney tissues (Fig. 3K). Next, we analyzed autophagy-related proteins, revealing disrupted autophagic flux owing to increased p62 levels, demonstrating failed cargo degradation. Our western blotting results of autophagy markers showed a significant increase in Beclin1 levels (Fig. 3B, $P < 0.001$) in Cd70 and Cd140 groups. Similarly, a marked elevation in the LC3B I/II ratio (Fig. 3C, $P < 0.001$) was observed in the Cd70 and Cd140, and notable increase levels ($P < 0.01$) were observed in the Cd35 group compared with the control group. Meanwhile, p62 levels were significantly increased (Fig. 3D, $P < 0.001$) in Cd35 and Cd70 and further elevated in Cd140 group ($P < 0.01$), indicated disrupted autophagic flux. The mRNA gene expression analysis results of *Beclin1, LC3B I/II,* and *P62* (Fig. 3 J, S3) were corroborated with the protein data findings.

Recent research has indicated a strong association between mitochondrial dynamics and autophagy. We conducted detailed analysis of mitochondrial dynamics (Fig. 3). The TEM micrographs revealed progressive mitochondrial damage in Cd-treated groups, while Con group showed normal morphology (Fig. 3K). Western blot results indicated significant changes in mitochondrial dynamics proteins, such as decreased levels of fusion proteins Mfn1, Mfn2, and OPA1 and elevated levels of fission protein markers Drp1 and Pink1 with Cd dose-dependent increase (Fig. 3A, 3F-I). PINK1, a crucial regulator of mitophagy, was significantly elevated (Fig. 3I, $P < 0.001$) in all Cd exposed groups, whereas Mfn2 promoted mitochondrial fusion, was significantly reduced in Cd70 and Cd140 (Fig. 3F, $P < 0.001$), indicating a shift toward mitochondrial fission and mitophagy. The mRNA gene expression analysis corroborated these findings, with upregulation of mitophagy-related genes (*PINK, DRP1, Fis1, BNIP3, FUNDC1*) and downregulation of fusion-related genes (*Mfn1, Mfn2, OPA1*) (Fig. 3J, S3). The heatmap of mRNA expression analysis results further supported evidence of mitochondrial dynamics and mitophagy impairment (Fig. 3 J, S3). Schematic illustration demonstrated that Cd caused mitochondrial dynamics and autophagy (Fig. 3L).

Nonetheless, significant mitochondrial damage in elevated Cd concentrations indicated that these protective mechanisms may be overwhelmed, potentially contributing to kidney damage.

Cd activated ATF4-CHOP transcriptional axis and inflammation

Cd exposure activated the CHOP-ATF4 transcriptional axis, an important mediator of ER-stress-triggered inflammation. IF staining revealed significant overexpression of ATF4 and CHOP in Cd140 (Fig. 4A–C, $P < 0.001$) in kidney tissues as compared to controls. This observation was confirmed by nuclear protein western blotting (Fig. 4D). In comparison with Con group, ATF4 and CHOP significantly exhibited elevated levels in the higher Cd140 group (Figs. 4E, 4F, $P < 0.001$). We analyzed the relative mRNA expressions of *ATF4* and *CHOP* and its downstream target genes, such as *ATF3, ERO1α*, and *NCR2C1*, the expressions were significantly upregulated in Cd exposure groups vs. Con (Fig. S4). These findings proved that Cd activated the ATF4-CHOP transcriptional axis, disrupting cellular homeostasis.

Cd exposure also activated inflammation, which plays a crucial role in tissue damage. The western blot analysis of the pro-inflammatory cytokine TNF-α showed a significant increase, whereas the anti-inflammatory cytokine IL-10 levels were significantly reduced in Cd70 and Cd140 groups (Fig. 4H, 4I, $P < 0.001$) respectively. Similarly, these findings were corroborated by mRNA results, which showed significant

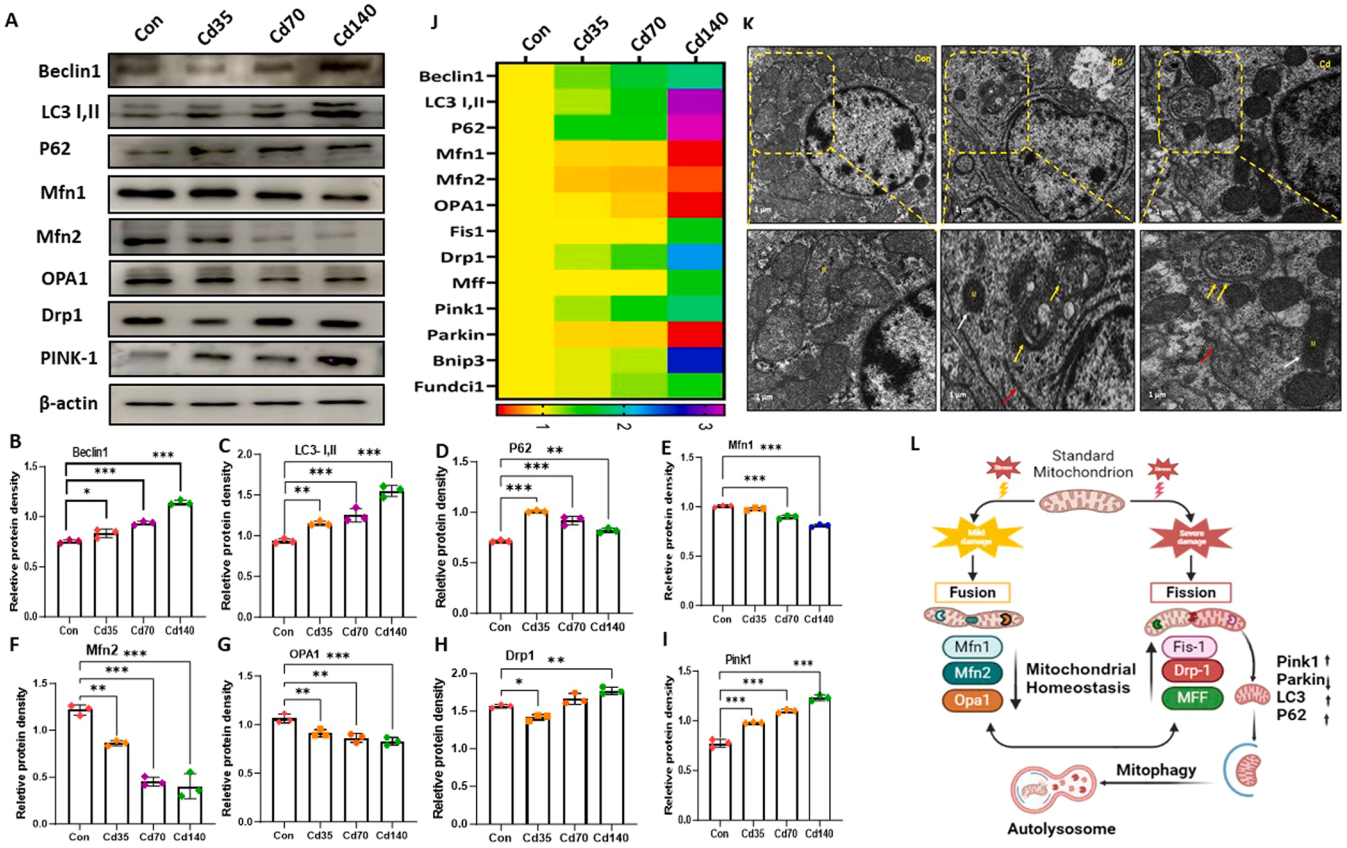

Fig. 3. Cd-induced mitochondrial dynamics and autophagy impairments. (A-I) Western blotting and calculation of relative protein densities of autophagy and mitochondrial dynamics-related proteins (Beclin-1, LC3β-I, II, P62, Mfn1, Mfn2, OPA1, Drp1, PINK1) in renal tissues. (J) qRT-PCR results demonstrated concordant changes in mRNA levels of autophagy mitochondrial dynamics and mitophagy-related genes (*Beclin-1, LC3β-I, II, P62, Mfn1, Mfn2, OPA1, Fis1, Drp1, MFF, PINK1, Parkin, BNIP3, FUNDC1*). (K) Transmission electron micrographs of kidney tissue from control and Cd-treated group. The white arrow represents mitochondria, the red arrow represents endoplasmic reticulum, and the yellow arrow represents autophagosomes (Scale bar: 1 μm). (L) The schematic illustration depicted the crosstalk between mitochondrial fission and fusion in Cd-induced-nephrotoxicity. Data are presented as mean ± SD. Symbols for the significance of difference between Con and Cd exposed groups: $^{*}P < 0.05$, $^{**}P < 0.01$, $^{***}P < 0.001$.

upregulation of pro-inflammatory mediators *TNF-α, IL-1β, NF-κB, iNOS, Cox-2*, and *IL-6* whereas downregulation of *IL-10* mRNA expressions in the Cd-exposed groups (Fig. S4). These findings indicated that Cd exposure exacerbated inflammation through ATF4-CHOP activation, contributing to cellular and tissue damage.

Effect of Cd exposure on renal apoptosis

Cd-triggered apoptosis is closely linked to ATF4-CHOP activation. The TUNEL assay showed a significant increase in apoptotic cells in Cd-treated group compared to Con (Fig. 5A and B, $P < 0.001$). Western blot analysis of key apoptotic markers supported this observation (Fig. 5C). We observed significant decreased anti-apoptotic protein Bcl2 levels in Cd70 ($P < 0.01$) and Cd140 groups (Fig. 5D - I, $P < 0.001$), whereas increased levels of pro-apoptotic proteins, including Bax, Bak, Casp-3, Casp-8, and Casp-9 in Cd70 ($P < 0.01$) and Cd140 groups (Fig. 5E–I, $P < 0.001$). Consistent with WB proteins data, mRNA analysis exhibited significant upregulation of pro-apoptotic genes *Bax, Bak, Casp-3, 8*, and *9,* while *Bcl2* was downregulated in Cd-exposed groups (Fig. S5). These results collectively indicated that Cd induced activation of the ATF4-CHOP transcriptional axis contributing to apoptosis, thereby exacerbating kidney damage.

Effect of Cd exposure on ATF4-CHOP and integrated pathways

We performed several integrated analyses to elucidate the intricate interactions between cellular pathways in Cd-induced renal damage. Correlations and PPI network of DEPs exhibited extensive interactions between ERstress, inflammation, mitochondrial dynamics mitophagy, leading to apoptosis (Fig. 6A, 6B). To further study the role of ATF4-CHOP in Cd-induced nephrotoxicity, we performed the protein-ligand docking analysis for ATF4-CHOP proteins with $CdCl_2$, and we found that the binding energy of ATF4 and CHOP proteins with $CdCl_2$ was -2.8 kcal/mol, indicating strong binding. All these results suggested Cd-induced apoptosis and renal dysfunction via ATF4-CHOP transcriptional complex (Fig. 6C).

Discussion

Cd is a widespread environmental toxic pollutant affecting human and animal health (Hamdan et al., 2024). Cd exposure mainly occurs through ingesting contaminated food and drinking water, inhaling polluted air and skin absorption (Zhu et al., 2024). This research executed toxicological studies on chickens and investigated the mechanisms of Cd-induced nephrotoxicity. Our results demonstrate that Cd-induced kidney damage is mediated via interdependent activation of ATF4-CHOP transcriptional axis, ER stress, mitochondrial dysfunction, impaired autophagy, and inflammation leading to apoptosis. This study established that ATF4-CHOP pathway is a crucial regulatory mechanism in Cd–induced nephrotoxicity and provides critical targets for therapeutic intervention in heavy metal-induced renal damage.

In recent years, several studies have explored the Cd nephrotoxic effects. The kidneys are the first target organ for Cd accumulation and damage (Alanazi et al., 2024; Schaefer et al., 2022). Cd exposure triggers

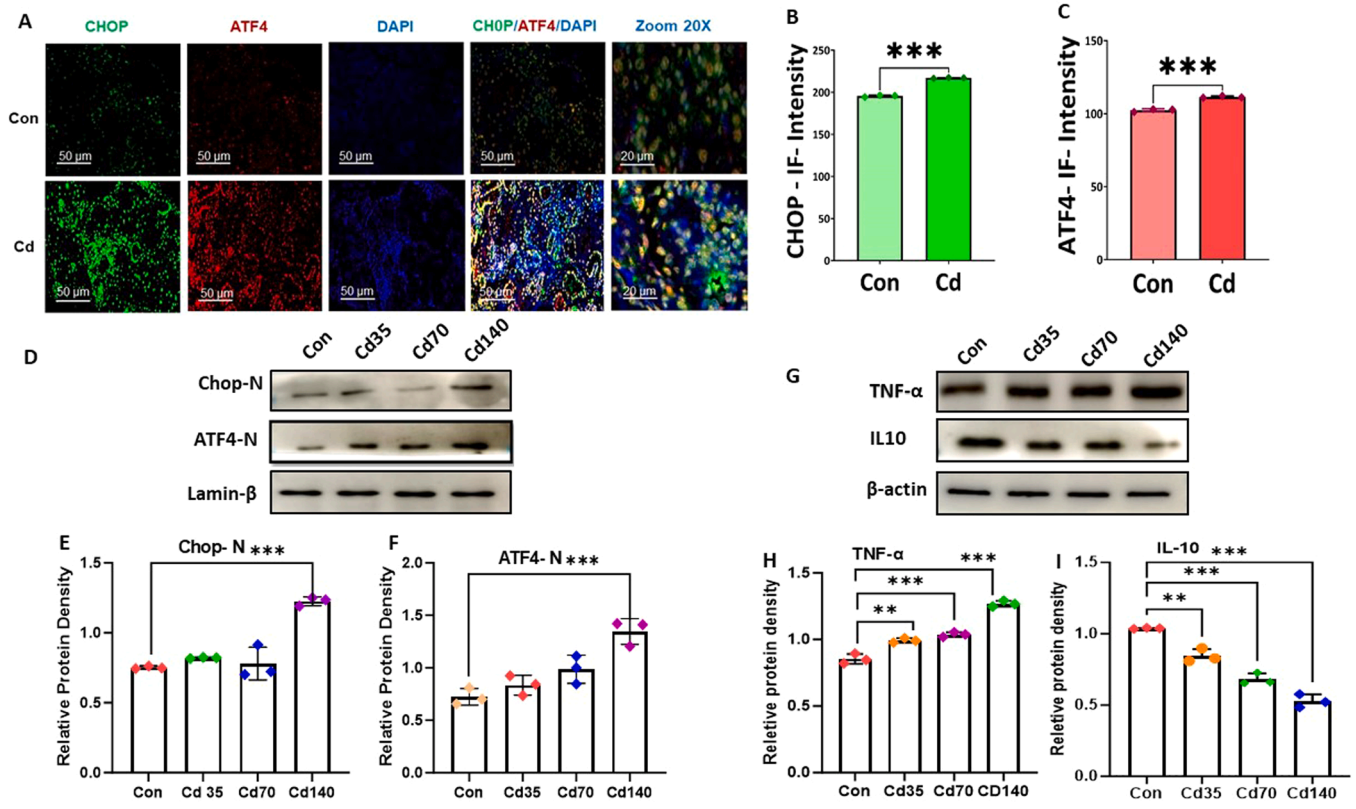

Fig. 4. Cadmium activated ATF4-CHOP transcriptional axis and inflammation. (A-C) IF of CHOP and ATF4 co-localization and IF intensities respectively. (D-F) Western blot analysis and quantification of nuclear proteins densities ATF4 and CHOP, Lamin B: nuclear loading. (G-I) Western blot protein levels and quantification of inflammatory markers: TNF-α, IL-10. Data are presented as mean ± SD. Symbols for the significance of difference between Con and Cd exposed groups: $^{*}P < 0.05$, $^{**}P < 0.01$, $^{***}P < 0.001$.

proximal renal tubular cell degeneration, glomerular atrophy, leukocyte infiltration, and impairment of Bowman's capsule. These histopathological changes may indicate renal damage in rats owing to Cd-induced excessive ROS production (Mohammedsaleh et al., 2024). Our H&E analysis showed that Cd exposure significantly increased tubular dilation and glomerular atrophy, these findings were corroborated by with previous research investigation, which revealed that Cd exposure triggers renal dysfunction through oxidative stress and structural damage (Gong et al., 2022; Lian et al., 2023). Furthermore, biochemical markers, including BUN, CREA, and UA, which serve as reliable indicators of renal function, were significantly elevated in Cd-treated groups indicated glomerular dysfunction, irregular excretion, and renal tissue damage (Novak et al., 2023). These biochemical disruptions align with previous research in various animal models (Ding et al., 2024; Kim et al., 2018; Salama et al., 2021; Śliwińska-Mossoń et al., 2019). BUN measures nitrogen from urea in the blood, with elevated levels demonstrating kidney impairment or dehydration. It has also eveloved as a biomarker for neurohormonal activation in heart failure, indicating renal responses beyond traditional role in renal function estimation (Kazory, 2010). CREA is a waste product of normal breakdown of muscle metabolism that, is filtered by the kidney and excreted in the urine. Serum CREA helps to estimate the glomerular filtration rate (GFR), a kidney function biomarker, with elevated levels suggesting reduced renal fuction (Fujii et al., 2022; Kim and Oh, 2022). UA is formed from purine breakdown, and elevated levels can cause gout, kidney stones, and renal impairment. UA levels increased in conditions such as hyperuricemic nephropathy and managing UA levels is crucial for preventing renal damage (Li et al., 2021a,b). In context of Cd exposure, elevated BUN, CREA, and UA levels indicate reduction in GFR, a hallmark of renal dysfunction. Biochemical indicators are essential markers for evaluating kidney fuction, each providing unique insights into renal health. Beyond their role in diagnosing kidney disease, these makers also have implications for broader health conditions, such as cardiovascular disease and heart failure. Consider their roles and interactions can help in the improved management and treatment of renal diseases (Hao et al., 2021; Pallio et al., 2019: Satarug et al., 2020). Oxidative stress plays important role in Cd-induced nephrotoxicity, as demonstrated by decreased antioxidant enzymes (CAT, SOD, and GSH) and elevated, which are usually lipid-peroxidation(MDA) (Ge et al., 2022) . ER stress is closely associated with oxidative stress and recognized as critical mechanism in Cd-Induced nephrotoxicity (Guo et al., 2022; Lian, Chu, Xia, Wang, Fan and Wang, 2023). ER is integral to protein folding, lipid production, and calcium storage, and its highly responsive to various external and intracellular stressor (Sengul et al., 2024). Cd exposure mainly targets the ER and induces ER stress (Li et al., 2021). GRP78/Bip is a specific molecular chaperone that ensures correct protein folding and transport under normal physiological conditions. Under chronic stress, it dissociates from transmembrane sensors and activates UPR to mitigate ER stress (Boulangé-Lecomte et al., 2014; Zhang et al., 2015). Cd-induced oxidative stress disrupts ER function, leading to the accumulation of misfolded proteins and activation of UPR (Zhang et al., 2023). Previous studies established that Cd treatment activated liver ER stress in a mouse model, and another research in chicken testes revealed Cd promotes the activation of IRE-1α, PERK, and JNK signaling pathways with upregulation of BIP/GRP78, ATF6, and CHOP proteins on the contrary (Zhang et al., 2023). Our previous study on chicken liver also confirmed that Cd exposure upregulates ER-stress proteins (Li et al., 2023). These findings are consistent with our results of ERstress-related proteins GRP78, elF2α, PERK1, IRE1α, ATF6, XBP1, and ATF4, CHOP that were upregulated in Cd treated groups (Fig. 2A), and mRNA expressions further supported our protein data results (Fig. S2). Collectively, we found that Cd-induced ER stress dysfunction overwhelms

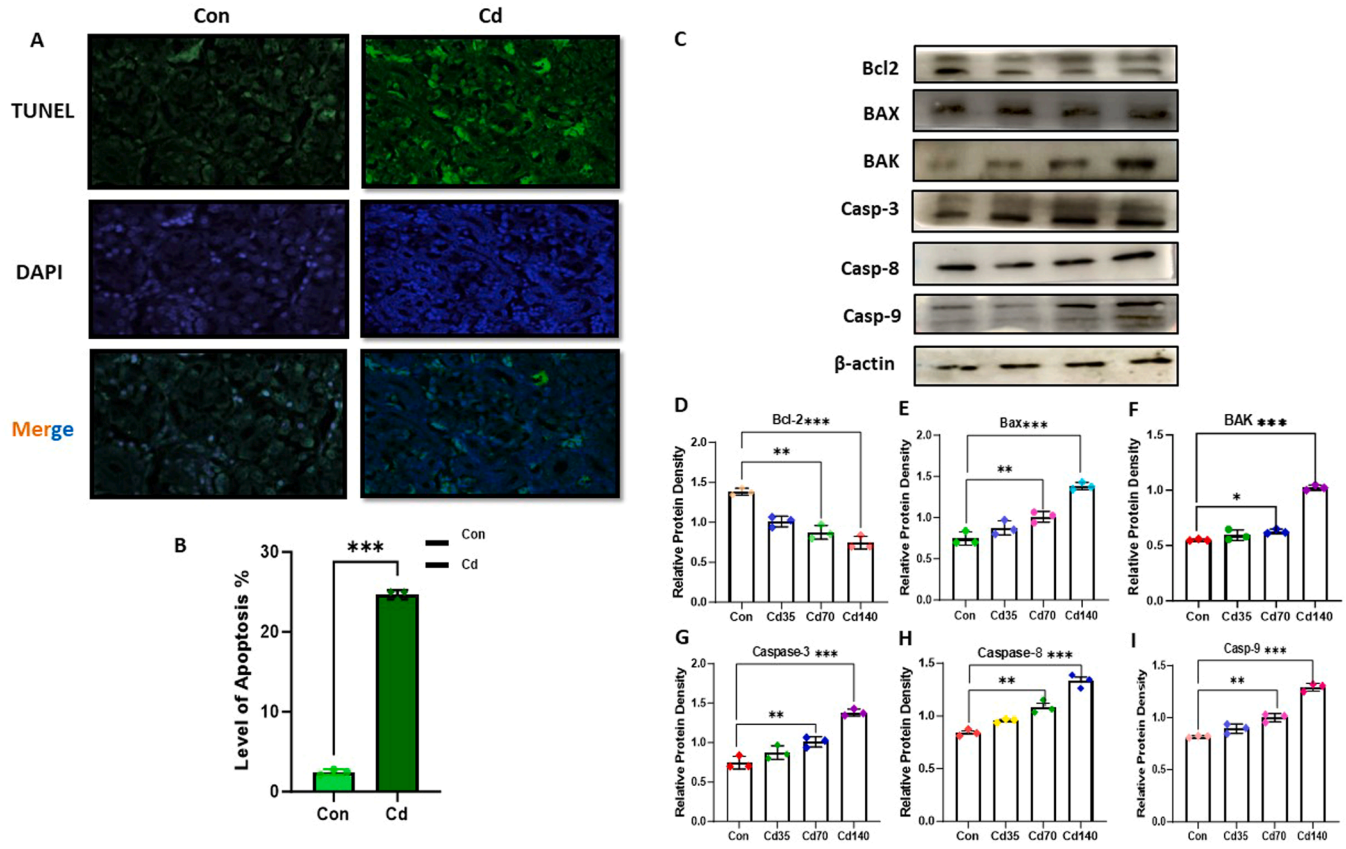

Fig. 5. Cadmium activated apoptosis. (A) TUNEL assay images, green: TUNEL-positive cells, blue: DAPI staining. (B) Quantification of TUNEL-positive cells. (C - I) Western blots and quantification of apoptotic markers Bcl2, Bax, Bak, Casp-3, Casp-8, and Casp-9. Data are presented as mean ± SD. Symbols for the significance in difference between Con and Cd exposed groups: $^{*}P < 0.05$, $^{**}P < 0.01$, $^{***}P < 0.001$.

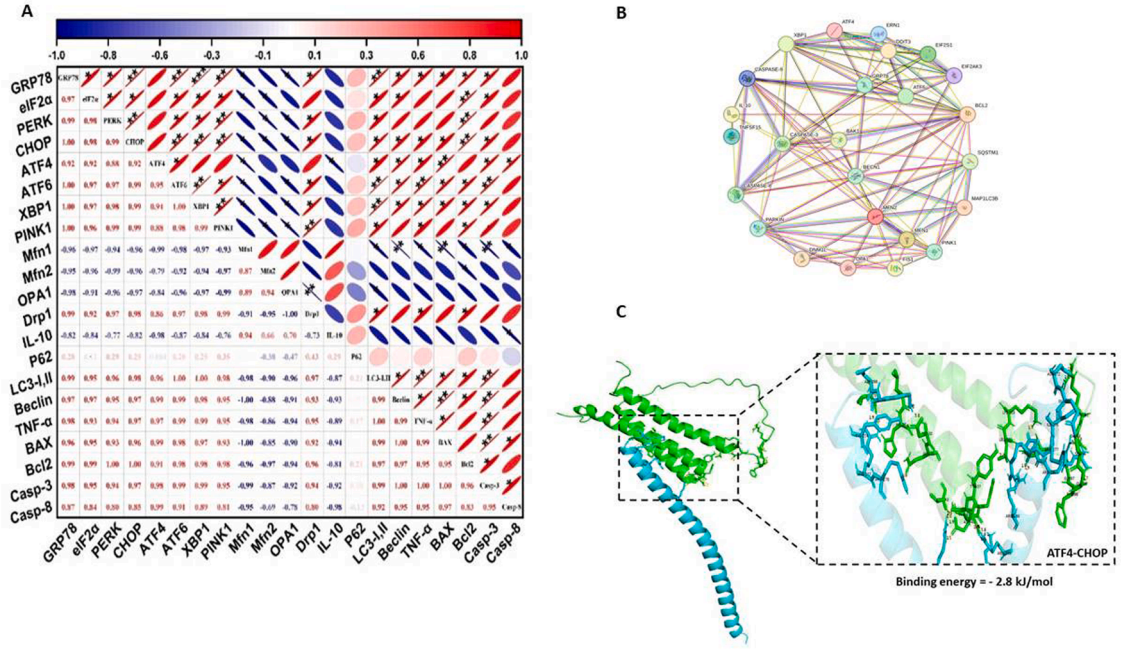

Fig. 6. Integrated analysis of pathways crosstalk in Cd- induced proximal renal tubular cell apoptosis. (A) Correlation analysis. (B) PPI network of differentially expressed genes, node size indicates degree of connectivity. (C) Molecular docking of protein-protein. Data are presented as mean ± SD. Symbols for the significance of difference between Con and Cd exposed groups: $^{*}P < 0.05$, $^{**}P < 0.01$, $^{***}P < 0.001$.

these adaptive mechanisms, contributing to cellular homeostasis disruption.

Autophagy is part of the intracellular protein degradation system and primarily facilitates the translocation of cytoplasmic organelles and misfolded proteins to lysosomes for degradation, which is significantly impaired by Cd exposure (Dong et al., 2024) . Our results indicated that Cd dysregulated autophagy, with increased proteins and mRNA levels of *LC3, Beclin1*, and *P62* (Fig. 3A–D), demonstrating altered autophagy flux. Our TEM analysis further revealed the accumulation of autophagosomes and damaged organelles in Cd-treated tissues, providing ultrastructural evidence of impaired autophagy. Previous studies have shown that autophagy and ER stress are interconnected via ATF4-CHOP axis (Wang et al., 2018; Zhao et al., 2021). Autophagy flux dysregulation leads to the accumulation of damaged organelles, aggravating oxidative stress, mitochondrial dysfunction, and apoptosis (Liu et al., 2017; Huang et al., 2025). TEM analysis revealed progressive mitochondrial damage, highlighting overwhelmed protective mechanisms leading to renal dysfunction in Cd-treated groups. Mitochondrial dynamics were disrupted by Cd exposure, with reduced expression of fusion proteins (Mfn1, Mfn2, OPA1) and increased fission proteins (Drp1, Pink1) (Kwon et al., 2023; Ni et al., 2023; Um et al., 2024). Dysfunctional mitochondria release cytochrome c into the cytoplasm, activating the apoptotic cascade via caspase-9 and caspase-3 (Huang, Ding, Ye, Wang, Yu, Yan, Liu and Wang, 2022; Tong et al., 2024). Mitochondrial dysfunction is associated with elevated ROS production, which accentuates oxidative stress, causing further damage to cellular structure and promoting ERstress and inflammation. This determines positive feedback where mitochondrial dysfunction exacerbates the stress response, ultimately leading to apoptosis (Feng et al., 2024). Recent study results further confirmed disrupted mitochondrial dynamics by reduced fusion proteins (Mfn1, Mfn2, OPA1) and increased fission-related protein levels (Dpr1, Pink1), which exacerbated oxidative stress and intensified ER stress in Cd-induced chicken kidneys (Fig. 7).

ATF4, a crucial regulator of ER stress, activates CHOP, initiating pro-apoptotic pathways. Recent studies indicated that ATF4 and CHOP increase protein synthesis, resulting in proteotoxicity, with CHOP-deficient mice, exhibiting resistance to pressure overload Cd–induced heart failure, whereas ATF4 overexpression facilitates cardiomyocytes death (Freundt et al., 2018; Jeong et al., 2019). ATF4-CHOP axis governs apoptosis and senescence in several cell types (Zou et al., 2024) . The ATF4-CHOP complex translocation emerges as a critical mechanism in Cd-induced renal toxicity. When Cd triggers PERK/elF2α pathway, ATF4 is activated and translocated to the nucleus (Cheng et al., 2024). Similarly, CHOP, a downstream target of ATF4, also translocates to the nucleus (Luo et al., 2016). This nuclear translocation enable the ATF4-CHOP complex to binds to specific DNA sequences, triggering complex cellular responses. Initially, these transcription factors promotes cell survival by activating the stress response and autophagy-related genes such as, *p62, NBr1* and *ATG7*. These genes help the cell's adaptive mechanisms to survive with Cd-induced stress. However, prolonged nuclear activation can shift the response towards pro-apoptotic gene expression. The complex regulates various cellular processes, such as oxidative stress resistance, mitochondrial function, and metabolic homeostasis. The nuclear ATF4-CHOP complex mediates a complex transcriptional mechanism balancing cellular adaption and potential cell death (B'chir et al., 2013; Fusakio et al., 2016; Mukherjee et al., 2020; Wortel et al., 2017). Our results demonstrated that Cd exposure activated the CHOP-ATF4 transcriptional axis, a key mediator of ERstress-triggered inflammation and apoptosis. IF staining revealed significant overexpression of both ATF4 and CHOP, further supported by nuclear protein results. Additionally, relative mRNA expression analysis exhibited upregulation of *ATF4* and *CHOP* and downstream target genes, such as *ATF3, ERO1α*, and *NCR2C1*, in Cd exposure groups vs. Con (Fig. S4). These findings prove that Cd activates the ATF4-CHOP transcriptional axis, disrupting cellular homeostasis. Cd exposure also activates inflammation, which plays a crucial role in tissue damage.

Apoptosis transpires as a result of dysregulation of apoptotic and anti-apoptotic proteins via mitochondrial-independent and dependent mechanisms (Sinha et al., 2013).The upregulation of Bax and down-regulation of Bcl2 expression significantly change the integrity of the mitochondrial membrane. Bax and Bcl2 facilitate the release of cytochrome c from mitochondria, which activates the basic apoptotic signaling cascade. Caspase-3 is recognized as a crucial apoptosis mediator as it triggers the execution of apoptotic mechanisms by activating other caspase enzymes. A previous investigation supported our research data that Cd treatment considerably elevated the levels of Caspase-3 and Bax and, decreased Bcl2 expression in rat renal tissues. Chronic Cd exposure upregulated Bax and Caspase-3 expression while reducing the levels of Bcl2 (Feng et al., 2024).

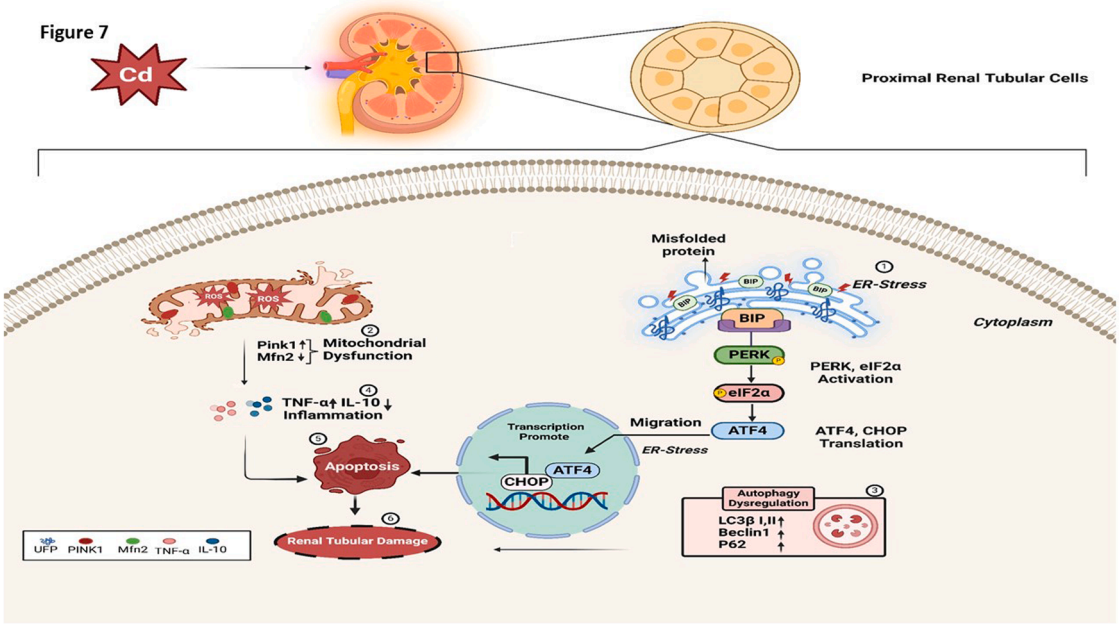

Fig. 7. Schematic diagram of cadmium disrupted homeostasis of proximal renal tubular cells via targeting ATF4-CHOP complex into the nucleus.

Conclusion

In conclusion, our results provide novel insights into the molecular mechanisms of Cd-induced nephrotoxicity in chickens. Cd exposure disrupts renal homeostasis and structure through several factors including oxidative stress, ER-stress, mitochondrial dysfunction, autophagy inhibition, inflammation, and apoptosis. Notably, ATF4-CHOP transcriptional complex emerges as a key mediator of associated pathways. This study highlights potential targets for future therapeutic interventions to mitigate the toxic effects of Cd in chickens. The specific molecular mechanisms and clinical significance of Cd-induced renal toxicity need to be further verified by cellular experiments.

Declaration of competing interest

All authors declared that they have no relevant interest relationships.

ACKNOWLEDGEMENTS

This research was supported by several funding sources, including the National Natural Science Foundation of China (Grant No. 32172932), Key Program of Natural Science Foundation of Heilongjiang Province of China (Grant No. ZD2021C003), China Agriculture Research System of MOF and MARA (No. CARS-35), Distinguished Professor of Longjiang Scholars Support Project (Grant No. T201908), and the Heilongjiang Touyan Innovation Team Program.

Supplementary materials

Supplementary material associated with this article can be found, in the online version, at doi:10.1016/j.psj.2025.105059.

References

Alanazi, S.T., Harisa, G.I., Salama, S.A., 2024. Modulating SIRT1, Nrf2, and NF-κb signaling pathways by bergenin ameliorates the cadmium-induced nephrotoxicity in rats. Chem. Biol. Interact. 387, 110797.

Ansari, M.A., Raish, M., Ahmad, A., Alkharfy, K.M., Ahmad, S.F., Attia, S.M., Alsaad, A. M., Bakheet, S.A., 2017. Sinapic acid ameliorate cadmium-induced nephrotoxicity: in vivo possible involvement of oxidative stress, apoptosis, and inflammation via NF-κb downregulation. Enviro. Toxicol. Pharmacol. 51, 100–107.

B'chir, W., Maurin, A.-C., Carraro, V., Averous, J., Jousse, C., Muranishi, Y., Parry, L., Stepien, G., Fafournoux, P., Bruhat, A., 2013. The eIF2α/ATF4 pathway is essential for stress-induced autophagy gene expression. Nucleic. Acids. Res. 41, 7683–7699.

Bautista, C.J., Arango, N., Plata, C., Mitre-Aguilar, I.B., Trujillo, J., Ramírez, V., 2024. Mechanism of cadmium-induced nephrotoxicity. Toxicology. 502, 153726.

Boulangé-Lecomte, C., Forget-Leray, J., Xuereb, B., 2014. Sexual dimorphism in Grp78 and Hsp90A heat shock protein expression in the estuarine copepod Eurytemora affinis. Cell Stress and Chaperones 19, 591–597.

Bronner, D.N., Abuaita, B.H., Chen, X., Fitzgerald, K.A., Nuñez, G., He, Y., Yin, X.-M., O'Riordan, M.X., 2015. Endoplasmic reticulum stress activates the inflammasome via NLRP3-and caspase-2-driven mitochondrial damage. Immunity. 43, 451–462.

Chen, M.-S., Wang, J.-X., Zhang, H., Cui, J.-G., Zhao, Y., Li, J.-L., 2023. Novel role of hemeoxygenase-1 in phthalate-induced renal proximal tubule cell ferroptosis. J. Agric. Food Chem. 71, 2579–2589.

Cheng, C., Yuan, Y., Yuan, F., Li, X., 2024. Acute kidney injury: exploring endoplasmic reticulum stress-mediated cell death. Front. Pharmacol. 15, 1308733.

Cui, J., Liu, Y., Hao, Z., Liu, Y., Qiu, M., Kang, L., Teng, X., Tang, Y., 2023. Cadmium induced time-dependent kidney injury in common carp via mitochondrial pathway: impaired mitochondrial energy metabolism and mitochondrion-dependent apoptosis. Aquat. Toxicol. 261, 106570.

Ding, L., Wang, K., Zhu, H., Liu, Z., Wang, J., 2024. Protective effect of quercetin on cadmium-induced kidney apoptosis in rats based on PERK signaling pathway. J. Trace Elem. Med. Biol. 82, 127355.

Doccioli, C., Sera, F., Francavilla, A., Cupisti, A., Biggeri, A., 2024. Association of cadmium environmental exposure with chronic kidney disease: a systematic review and meta-analysis. Sci. Total. Environ. 906, 167165.

Dong, P.-F., T.-B. Liu, K. Chen, D. Li, Y. Li, C.-Y. Lian, Z.-Y. Wang, and L. Wang. 2024. Cadmium targeting transcription factor EB to inhibit autophagy-lysosome function contributes to acute kidney injury. J. Adv. Res.. S2090123224002972.

Feng, R., Wang, D., Li, T., Liu, X., Peng, T., Liu, M., Ren, G., Xu, H., Luo, H., Lu, D., 2024. Elevated SLC40A1 impairs cardiac function and exacerbates mitochondrial dysfunction, oxidative stress, and apoptosis in ischemic myocardia. Int. J. Biol. Sci. 20, 414.

Freundt, J.K., Frommeyer, G., Wötzel, F., Huge, A., Hoffmeier, A., Martens, S., Eckardt, L., Lange, P.S., 2018. The transcription factor ATF4 promotes expression of cell stress genes and cardiomyocyte death in a cellular model of atrial fibrillation. Biomed. Res. Int., 3694362, 2018.

Fujii, R., Melotti, R., Gögele, M., Barin, L., Ghasemi-Semeskandeh, D., Barbieri, G., Pramstaller, P.P., Pattaro, C., 2022. Structural equation modeling of kidney function biomarkers improves incident cardiovascular risk estimation: TH-PO624. Journal of the American Society of Nephrology 33, 224.

Fujiki, K., Tanabe, K., Suzuki, S., Mochizuki, A., Mochizuki-Kashio, M., Sugaya, T., Mizoguchi, T., Itoh, M., Nakamura-Ishizu, A., Inamura, H., 2024. Blockage of Akt activation suppresses cadmium-induced renal tubular cellular damages through aggrephagy in HK-2 cells. Sci. Rep. 14, 14552.

Fusakio, M.E., Willy, J.A., Wang, Y., Mirek, E.T., Al Baghdadi, R.J., Adams, C.M., Anthony, T.G., Wek, R.C., 2016. Transcription factor ATF4 directs basal and stress-induced gene expression in the unfolded protein response and cholesterol metabolism in the liver. Mol. Biol. Cell 27, 1536–1551.

Ge, J., Huang, Y., Lv, M., Zhang, C., Talukder, M., Li, J., Li, J., 2022. Cadmium induced Fak-mediated anoikis activation in kidney via nuclear receptors (AHR/CAR/PXR)-mediated xenobiotic detoxification pathway. J. Inorg. Biochem. 227, 111682.

Gong, Z.-G., Zhao, Y., Wang, Z.-Y., Fan, R.-F., Liu, Z.-P., Wang, L., 2022. Epigenetic regulator BRD4 is involved in cadmium-induced acute kidney injury via contributing to lysosomal dysfunction, autophagy blockade and oxidative stress. J. Hazard. Mater. 423, 127110.

Gu, J., Dai, S., Liu, Y., Liu, H., Zhang, Y., Ji, X., Yu, F., Zhou, Y., Chen, L., Tse, W.K.F., 2018. Activation of Ca2+-sensing receptor as a protective pathway to reduce Cadmium-induced cytotoxicity in renal proximal tubular cells. Sci. Rep. 8, 1092.

Guo, H., Hu, R., Huang, G., Pu, W., Chu, X., Xing, C., Zhang, C., 2022. Molybdenum and cadmium co-exposure induces endoplasmic reticulum stress-mediated apoptosis by Th1 polarization in Shaoxing duck (Anas platyrhyncha) spleens. Chemosphere 298, 134275.

Guo, Y.-Y., Liang, N.-N., Zhang, X.-Y., Ren, Y.-H., Wu, W.-Z., Liu, Z.-B., He, Y.-Z., Zhang, Y.-H., Huang, Y.-C., Zhang, T., 2024. Mitochondrial GPX4 acetylation is involved in cadmium-induced renal cell ferroptosis. Redox. Biol. 73, 103179.

Hamdan, Y.A., Baba, A.A., Azraida, H., Kabdy, H., Oudadesse, H., Chait, A., Rhazi, M., 2024. In vivo evaluation by oral administration of chitosan combined with bioactive glass against cadmium-induced toxicity in rats. J. Inorg. Biochem. 276, 133845.

Hao, R., Song, X., Sun-Waterhouse, D., Tan, X., Li, F., Li, D., 2021. MiR-34a/Sirt1/p53 signaling pathway contributes to cadmium-induced nephrotoxicity: a preclinical study in mice. Environmental Pollution 282, 117029.

Huang, R., Ding, L., Ye, Y., Wang, K., Yu, W., Yan, B., Liu, Z., Wang, J., 2022. Protective effect of quercetin on cadmium-induced renal apoptosis through cyt-c/caspase-9/caspase-3 signaling pathway. Front. Pharmacol. 13, 990993.

Huang, X.-R., L, Y.e., An, N., Wu, C.-Y., Wu, H.-L., Li, H.-Y., Huang, Y.-H., Ye, Q.-R., Liu, M.-D., Yang, L.-W., 2025. Macrophage autophagy protects against acute kidney injury by inhibiting renal inflammation through the degradation of TARM1. Autophagy. 21, 120–140.

Ijaz, M.U., Shahzadi, S., Hamza, A., Azmat, R., Anwar, H., Afsar, T., Shafique, H., Bhat, M.A., Naglah, A.M., Al-Omar, M.A., 2023. Alleviative effects of pinostrobin against cadmium-induced renal toxicity in rats by reducing oxidative stress, apoptosis, inflammation, and mitochondrial dysfunction. Front. Nutrit. 10, 1175008.

Jeong, M.-H., Jeong, H.-J., Ahn, B.-Y., Pyun, J.-H., Kwon, I., Cho, H., Kang, J.-S., 2019. PRMT1 suppresses ATF4-mediated endoplasmic reticulum response in cardiomyocytes. Cell Death. Dis. 10, 903.

Jiang, F.-W., Guo, J.-Y., Lin, J., Zhu, S.-Y., Dai, X.-Y., Saleem, M.A.U., Zhao, Y., Li, J.-L., 2024. Mapk/nf-κb signaling mediates atrazine-induced cardiorenal syndrome and antagonism of lycopene. Sci. Total. Environ. 922, 171015.

Jung, K.-T., Oh, S.-H., 2022. The role of autophagy in cadmium-induced acute toxicity in glomerular mesangial cells and tracking polyubiquitination of cytoplasmic p53 as a biomarker. Exp. Mol. Med. 54, 685–696.

Kaya, S., Yalçın, T., 2024. Linalool may have a therapeutic effect on cadmium-induced nephrotoxicity by regulating NF-κb/TNF and GRP78/CHOP signaling pathways. J. Trace Elem. Med. Biol. 86, 127510.

Kazory, A., 2010. Emergence of blood urea nitrogen as a biomarker of neurohormonal activation in heart failure. Am. J. Cardiol. 106, 694–700.

Kim, J.H., Oh, K.-H., 2022. Comparison of cardiovascular event predictability between the 2009 CKD-EPI equation and the new 2021 CKD-EPI equations in a Korean CKD cohort: from the KNOW-CKD study: TH-PO623. Journal of the American Society of Nephrology 33, 224.

Kim, K.S., Lim, H.-J., Lim, J.S., Son, J.Y., Lee, J., Lee, B.M., Chang, S.-C., Kim, H.S., 2018. Curcumin ameliorates cadmium-induced nephrotoxicity in Sprague-Dawley rats. Food Chem. Toxicol. 114, 34–40.

Kwon, J., Kim, J., Kim, K.I., 2023. Crosstalk between endoplasmic reticulum stress response and autophagy in human diseases. Anim. Cell. Syst. 27, 29–37.

Li, X.-W., Li, S., Yang, Y., Milton Talukder, Xu, X.-W., Li, C.-X., Zhang, C., Li, X.-N., 2024. The FAK/occludin/ZO-1 complex is critical for cadmium-induced testicular damage by disruption of the integrity of the blood-testis barrier in chickens. J. hazard. mater. 470, 134126.

Li, D., Yang, C., Sun, L., Zhao, Z., Liu, J., Zhang, C., Sun, D., Zhang, Q., 2024. High fluoride aggravates cadmium-mediated nephrotoxicity of renal tubular epithelial cells through ROS-PINK1/Parkin pathway. Sci. Total. Environ. 953, 175927.

Li, L., Cheng, D., An, X., Liao, G., Zhong, L., Liu, J., Chen, Y., Yuan, Y., Lu, Y., 2021a. Mesenchymal stem cells transplantation attenuates hyperuricemic nephropathy in rats. Int. Immunopharmacol. 99, 108000.

Li, L., Li, Y., Luo, J., Jiang, Y., Zhao, Z., Chen, Y., Huang, Q., Zhang, L., Wu, T., Pang, J., 2021b. Resveratrol, a novel inhibitor of GLUT9, ameliorates liver and kidney injuries in ad-galactose-induced ageing mouse model via the regulation of uric acid metabolism. Food Funct. 12, 8274–8287.

Li, N., Yi, B.-J., Saleem, M.A.U., Li, X.-N., Li, J.-L., 2023. Autophagy protects against Cd-induced cell damage in primary chicken hepatocytes via mitigation of oxidative stress and endoplasmic reticulum stress. Ecotoxicol. Environ. Saf. 259, 115056.
Li, X., Ge, M., Zhu, W., Wang, P., Wang, J., Tai, T., Wang, Y., Sun, J., Shi, G., 2021. Protective effects of astilbin against cadmium-induced apoptosis in chicken kidneys via endoplasmic reticulum stress signaling pathway. Biol. Trace Elem. Res. 1–14.
Lian, C.-Y., Chu, B.-X., Xia, W.-H., Wang, Z.-Y., Fan, R.-F., Wang, L., 2023. Persistent activation of Nrf2 in a p62-dependent non-canonical manner aggravates lead-induced kidney injury by promoting apoptosis and inhibiting autophagy. J. Adv. Res. 46, 87–100.
Liu, F., Wang, X.-Y., Zhou, X.-P., Liu, Z.-P., Song, X.-B., Wang, Z.-Y., Wang, L., 2017. Cadmium disrupts autophagic flux by inhibiting cytosolic Ca2+-dependent autophagosome-lysosome fusion in primary rat proximal tubular cells. Toxicology. 383, 13–23.
Luo, B., Lin, Y., Jiang, S., Huang, L., Yao, H., Zhuang, Q., Zhao, R., Liu, H., He, C., Lin, Z., 2016. Endoplasmic reticulum stress eIF2α–ATF4 pathway-mediated cyclooxygenase-2 induction regulates cadmium-induced autophagy in kidney. Cell Death. Dis. 7 e2251-e2251.
Ma, Y., Su, Q., Yue, C., Zou, H., Zhu, J., Zhao, H., Song, R., Liu, Z., 2022. The effect of oxidative stress-induced autophagy by cadmium exposure in kidney, liver, and bone damage, and neurotoxicity. IJOMS 23, 13491.
Mohammedsaleh, Z.M., Hassanein, E.H., Ali, F.E., Althagafy, H.S., Al-Abbas, N.S., Atwa, A.M., 2024. Perindopril dampens Cd-induced nephrotoxicity by suppressing inflammatory burden, Ang II/Ang 1–7, and apoptosis signaling pathways. Biol. Trace Elem. Res. 202, 3193–3203.
Mori, C., Lee, J.-Y., Tokumoto, M., Satoh, M., 2022. Cadmium toxicity is regulated by peroxisome proliferator-activated receptor δ in human proximal tubular cells. IJMS 23, 8652.
Mukherjee, D., Bercz, L.S., Torok, M.A., Mace, T.A., 2020. Regulation of cellular immunity by activating transcription factor 4. Immunol. Lett. 228, 24–34.
Ni, H., Ou, Z., Wang, Y., Liu, Y., Sun, K., Zhang, J., Zhang, J., Deng, W., Zeng, W., Xia, R., 2023. XBP1 modulates endoplasmic reticulum and mitochondria crosstalk via regulating NLRP3 in renal ischemia/reperfusion injury. Cell Death. Discov. 9, 69.
No, R., 2021. 1372 of 17 August 2021 amending annex IV to Regulation (EC) No 999/2001 of the European Parliament and of the Council as regards the prohibition to feed non-ruminant farmed animals, other than fur animals, with protein derived from animals text with EEA relevance. Off J Eur Union 1–17.
Novak, R., Salai, G., Hrkac, S., Vojtusek, I.K., Grgurevic, L., 2023. Revisiting the role of NAG across the continuum of Kidney disease. Bioengineering 10, 444.
Pallio, G., Micali, A., Benvenga, S., Antonelli, A., Marini, H.R., Puzzolo, D., Macaione, V., Trichilo, V., Santoro, G., Irrera, N., 2019. Myo-inositol in the protection from cadmium-induced toxicity in mice kidney: an emerging nutraceutical challenge. Food and Chemical Toxicology 132, 110675.
Rahman, S.U., Han, J.-C., Ahmad, M., Gao, S., Khan, K.A., Li, B., Zhou, Y., Zhao, X., Huang, Y., 2023. Toxic effects of lead (Pb), cadmium (Cd) and tetracycline (TC) on the growth and development of Triticum aestivum: a meta-analysis. Sci. Total. Environ., 166677
Salama, S.A., Mohamadin, A.M., Abdel-Bakky, M.S., 2021. Arctigenin alleviates cadmium-induced nephrotoxicity: targeting endoplasmic reticulum stress, Nrf2 signaling, and the associated inflammatory response. Life Sci. 287, 120121.
Satarug, S., Gobe, G., Ujjin, P., Vesey, D., 2020. A comparison of the nephrotoxicity of low doses of cadmium and lead. Toxics. 8 (1), 18.
Schaefer, H.R., Flannery, B.M., Crosby, L., Jones-Dominic, O.E., Punzalan, C., Middleton, K., 2022. A systematic review of adverse health effects associated with oral cadmium exposure. Regul. Toxicol. Pharmacol. 134, 105243.
Sengul, E., Yildirim, S., Cinar, İ., Tekin, S., Dag, Y., Bolat, M., Gok, M., Warda, M., 2024. Mitigation of acute hepatotoxicity induced by cadmium through morin: modulation of oxidative and pro-apoptotic endoplasmic reticulum stress and inflammatory responses in rats. Biol. Trace Elem. Res. 1–12.
Sinha, K., Das, J., Pal, P.B., Sil, P.C., 2013. Oxidative stress: the mitochondria-dependent and mitochondria-independent pathways of apoptosis. Arch. of Toxicol. 87, 1157–1180.
Śliwińska-Mossoń, M., Sobiech, K., Dolezych, B., Madej, P., Milnerowicz, H., 2019. N-acetyl-beta-D-glucosaminidase in tissues of rats chronically exposed to cadmium and treated with ozone. Annal. Clinic. Lab. Sci 49, 193–203.
Sun, X.-H., Lv, M.-W., Zhao, Y.-X., Zhang, H., Ullah Saleem, M.A., Zhao, Y., Li, J.-L., 2022. Nano-selenium antagonized cadmium-induced liver fibrosis in chicken. J. Agri. Food Chem. 71, 846–856.
Talukder, M., Bi, S.-S., Jin, H.-T., Ge, J., Zhang, C., Lv, M.-W., Li, J.-L., 2021. Cadmium induced cerebral toxicity via modulating MTF1-MTs regulatory axis. Environ. Pollution. 285, 117083.
Tong, X., Wang, G., Zhao, X., Zhou, J., Wang, P., Xia, H., Bian, J., Liu, X., Yuan, Y., Zou, H., 2024. Angelica sinensis polysaccharides mitigate cadmium-induced apoptosis in layer chicken chondrocytes by inhibiting the JNK signaling pathway. Int. J. Biol. Macromol. 282, 137106.
Um, J.-H., Shin, D.J., Choi, S.M., Nathan, A.B.P., Kim, Y.Y., Jeong, D.J., Kim, D.H., Kim, K.H., Kim, Y.H., Nah, J., 2024. Selective induction of Rab9-dependent alternative mitophagy using a synthetic derivative of isoquinoline alleviates mitochondrial dysfunction and cognitive deficits in Alzheimer's disease models. Theranostics. 14, 56.
Vesey, D.A., 2010. Transport pathways for cadmium in the intestine and kidney proximal tubule: focus on the interaction with essential metals. Toxicol. Lett. 198, 13–19.
Wang, J., Qi, Q., Zhou, W., Feng, Z., Huang, B., Chen, A., Zhang, D., Li, W., Zhang, Q., Jiang, Z., 2018. Inhibition of glioma growth by flavokawain B is mediated through endoplasmic reticulum stress induced autophagy. Autophagy. 14, 2007–2022.
Wortel, I.M., van der Meer, L.T., Kilberg, M.S., van Leeuwen, F.N., 2017. Surviving stress: modulation of ATF4-mediated stress responses in normal and malignant cells. Trends in Endocrinology & Metabolism 28, 794–806.
Wróblewski, K., Wojnicka, J., Tutka, P., Szmagara, A., Błażewicz, A., 2024. Measurements of cadmium levels in relation to tobacco dependence and as a function of cytisine administration. Sci. Rep. 14, 1883.
Wu, D., Huang, L.-F., Chen, X.-C., Huang, X.-R., Li, H.-Y., An, N., Tang, J.-X., Liu, H.-F., Yang, C., 2023. Research progress on endoplasmic reticulum homeostasis in kidney diseases. Cell Death. Dis. 14, 473.
Zhang, B., Liu, Y., Zhang, J.-S., Zhang, X.-H., Chen, W.-J., Yin, X.-H., Qi, Y.-F., 2015. Cortistatin protects myocardium from endoplasmic reticulum stress induced apoptosis during sepsis. Mol. Cell Endocrinol. 406, 40–48.
Zhang, J., Yang, W., Li, Z., Huang, F., Zhang, K., 2023. Multigenerational exposure of cadmium trans-generationally impairs locomotive and chemotactic behaviors in Caenorhabditis elegans. Chemosphere 325, 138432.
Zhang, K., Li, J., Dong, W., Huang, Q., Wang, X., Deng, K., Ali, W., Song, R., Zou, H., Ran, D., 2024a. Luteolin alleviates cadmium-induced kidney injury by inhibiting oxidative DNA damage and repairing autophagic flux blockade in chickens. Antioxidants 13, 525.
Zhang, W., Shi, Y., Oyang, L., Cui, S., Li, S., Li, J., Liu, L., Li, Y., Peng, M., Tan, S., 2024b. Endoplasmic reticulum stress—A key guardian in cancer. Cell Death Discovey 10, 343.
Zhao, C., Yu, D., He, Z., Bao, L., Feng, L., Chen, L., Liu, Z., Hu, X., Zhang, N., Wang, T., 2021. Endoplasmic reticulum stress-mediated autophagy activation is involved in cadmium-induced ferroptosis of renal tubular epithelial cells. Free Radic. Biomed. 175, 236–248.
Zhao, M., Xie, L., Huang, W., Li, M., Gu, X., Zhang, W., Wei, J., Zhang, N., 2024. Combined effects of cadmium and lead on growth performance and kidney function in broiler chicken. Biol.Trace Elem. Res. 1–16.
Zhao, Y.-X., Li, X.-N., Tang, Y.-X., Talukder, M., Zhao, Y., Li, J.-L., 2023. Cadmium transforms astrocytes into the A1 subtype via inducing gap junction protein connexin 43 into the nucleus. J. Agri Food Chem. 71, 12043–12051.
Zhu, H., Tang, X., Gu, C., Chen, R., Liu, Y., Chu, H., Zhang, Z., 2024. Assessment of human exposure to cadmium and its nephrotoxicity in the Chinese population. Sci. Total. Environ., 170488
Zou, L., Wang, Y., Hu, Y., Liu, L., Luo, L., Chen, Z., Zhuo, Y., Li, P., Zhou, Q., 2024. N-cadherin alleviates apoptosis and senescence of nucleus pulposus cells via suppressing ROS-dependent ERS in the hyper-osmolarity. Int. J. Med. Sci. 21, 341.